

Piezoelectricity in gadolinium ferrite: A computational study

Marcos Antonio B dos Santos¹, Márcio de Souza Farias², Fábio dos Santos Gil², Antônio Florêncio de Figueiredo³, Raimundo D de Paula Ferreira², Helieverton Geraldo de Brito², Luã Felipe de Oliveira¹, Hérica Coelho Cordeiro¹, Oswaldo Treu-Filho², José Ciríaco-Pinheiro²

¹Departamento de Ciências Naturais, Universidade do Estado do Pará, Campus de Barcarena, PA, Brasil, CEP 68477-00

²Laboratório de Química Teórica e Computacional, Instituto de Ciências Exatas e Naturais, Faculdade de Química, Universidade Federal do Pará, Belém, PA, Brasil, CEP 66075-110

³Instituto Federal de Educação, Ciência e Tecnologia do Pará, Campus de Castanhal, PA, Brasil, CEP 68741-970

*Corresponding author (J. Ciríaco-Pinheiro), E-mail: ciriaco@ufpa.br

Abstract— Douglas-Koll-Hess (DKH) second-order relativistic scalar approach was used to investigate piezoelectricity in gadolinium ferrite (GdFeO_3). To adequately represent the polyatomic environment studied – ($24s13p$), ($29s17p12d$) and ($32s22p16d10f$)– basis sets were built for the atoms O (3P), Fe (5D), and Gd (9D), then contracted to [$4s2p$], [$12s6p5d$], and [$19s12p8d4f$], respectively. The qualifying of the contracted basis sets for GdFeO_3 crystal studies was conducted in three moments, namely: quality evaluation in molecular calculations, made in $^1\text{FeO}^{1+}$ and $^1\text{GdO}^{1+}$ molecular fragments; the choice of polarization function used in the [$4s2p$] basis set for O (3P) atom; the choice of diffuse functions used in the [$12s6p5d$] and [$19s12p8d4f$] basis sets for Fe (5D) and Gd (9D) atoms, respectively. The qualified contracted basis sets gave rise to the molecular [$4s2p1d$]/[$13s7p6$]/[$20s13p9d5f$] basis set which was then used to describe geometric parameters of the GdFeO_3 crystal. The good performance of the [$4s2p1d$]/[$13s7p6$]/[$20s13p9d5f$] basis set in describing the geometry of the material of interest led to calculations of the material properties: total relativistic energy, dipole moment and total atomic charge. The analysis of the results for these properties showed that the possible piezoelectricity in GdFeO_3 can be caused by electrostatic interactions of its atoms.

Keywords— Piezoelectricity, Gadolinium ferrite, Qualified basis sets, Computational study, Perovskite.

I. INTRODUCTION

Since the discovery of the piezoelectric effect on Barium Titanate (BaTiO_3) ceramics by Roberts in 1947 [1], a large number of perovskite oxides presenting this property have been obtained. Perovskites are of great interest in materials science because they are relatively simple crystalline structures and exhibit many properties such as electrical, magnetic, optical, and catalytic properties among others [2-7].

Certain crystalline materials have the ability to develop an electric charge proportional to a mechanical stress called piezoelectricity. It has been realized that materials showing this phenomenon must also show the converse, a geometric strain (deformation) proportional to an applied voltage [8].

The perovskite structure is a network of corner linked oxygen octahedra, with the smaller cations filling the octahedral holes and the large cations filling the dodecahedral holes [9]. The piezoelectric properties in perovskite structure result from uncentrosymmetric characteristics [10].

We have reported in the literature computational investigations on piezoelectric properties in perovskites. In these studies, the importance of the set of atomic bases developed exclusively to adequately represent the polyatomic environment has been pointed out [11, 12]. The details of this subject can be found elsewhere [13].

Results from the theory can help experimentalists better design their experiments to rationalize the use of time and resources to study a system under investigation.

The aim of this study is to provide some insight into the investigation of gadolinium ferrite (GdFeO_3) piezoelectricity through the use of quantum mechanics.

The very-well documented generator coordinate Hartree-Fock (GCHF) method [13-16] was used to build (24s13p), (29s17p12d), and (32s22p16d10f) basis sets for O (^3P), Fe (^5D), and Gd (^9D) atoms, respectively, which were contracted to [4s2p], [12s6p5d], and [19s12p8d4f], evaluated in molecular calculations, and then after supplementation of these sets with polarization functions and diffuse functions, to adequately represent the polydomic environment of the GdFeO_3 crystal, through a good description of the total energy and the energies of the HOMO (highest occupied molecular orbital) and HOMO-1 orbitals (one level below to highest occupied molecular orbital). Lastly, contracted and supplemented basis sets with polarization function and diffuse functions were used in the quantum-mechanical study of piezoelectricity in GdFeO_3 at DKH second-order relativistic scalar level [17-19].

II. COMPUTATIONAL METHODOLOGY

Details about the formalism as well as the strategies used by GCHF approach in the construction of basis sets are given in Refs. [14-16]. In this section, we describe the procedures used in constructing the contracted basis sets and qualifying the contracted basis sets for the study of piezoelectricity in GdFeO_3 .

Full details about all wave functions generated in this work are available by e-mailing to: ciriaco@ufpa.br.

The contractions of the (24s13p)/[4s2p], (29s17p12d)/[12s6p5d], and (32s22p16d10f)/[19s12p8d4f] basis sets were carried out with the segmented contraction

scheme [20] as follows: [4s2p] (16, 4, 3, 1/12, 1); [12s6p5d] (10, 3, 2, 1, 1, 1, 2, 2, 2, 2, 2, 1/5, 5, 3, 2, 1, 1/8, 1, 1, 1, 1); [19s12p8d4f] (11, 2, 2, 2, 1, 1, 1, 1, 1, 1, 1, 1, 1, 1, 1, 1, 1/9, 3, 1, 1, 1, 1, 1, 1, 1, 1/6, 4, 1, 1, 1, 1, 1, 1/7, 1, 1, 1).

The qualification procedure of the contracted basis sets was performed in three moments, as follows: quality evaluation of the contracted basis sets in molecular calculations with the $^1\text{FeO}^{1+}$ and $^1\text{GdO}^{1+}$ molecular fragments; the choice of polarization function used in the contracted basis set for the O (^3P) atom; the choice of diffuse functions used in the contracted basis sets for the Fe (^5D) and Gd (^9D) atoms. These three moments will be detailed below:

DKH second-order scalar relativistic [17-19] calculations were performed for the TRE (total relativistic energy), the HOMO (highest occupied molecular orbital theory) energy, and the HOMO-1 (one-level below to highest occupied molecular orbital) energy for $^1\text{FeO}^{1+}$ and $^1\text{GdO}^{1+}$ fragments in order to evaluate the quality of contracted basis sets in the representation of molecular environments. The quality of these calculations was compared to that obtained with the basis sets (24s13p), (29s17p12d), and (32s22p16d10f).

TABLE 1 shows the TRE, the HOMO, and the HOMO-1 energies for the fragments. According to this table, it can be noted that the TRE, the HOMO and HOMO-1 energies obtained with the contracted basis sets are close to those obtained with the uncontracted basis sets. The differences in the TRE are 0.129 and 1.09 hartree for $^1\text{FeO}^{1+}$ and $^1\text{GdO}^{1+}$, respectively. The HOMO energy shows a difference of 5.0×10^{-3} hartree for the two fragments. While for the HOMO-1 energy the differences are 2.0×10^{-3} and 1.0×10^{-2} hartree.

Table 1. TER, HOMO energy and HOMO-1 energy (hartree) for the $^1\text{FeO}^{1+}$ and $^1\text{GdO}^{1+}$ molecular fragments

Molecular fragment	Basis sets	TRE	HOMO energy	HOMO-1 energy
$^1\text{FeO}^{1+}$	[12s6p5d] ¹ /[4s2p] ²	-1336.314429	-0.281	-0.663
	(29s17p12d) ³ /(24s13p) ⁴	-1336.443455	-0.286	-0.665
$^1\text{GdO}^{1+}$	[19s12p8d4f] ⁵ /[4s2p] ²	-10892.24445	-0.219	-0.569
	(32s22p16d10f) ⁶ /(24s13p) ⁴	-10893.33562	-0.224	-0.579

^{1,3}Contracted and uncontracted basis sets for Fe (^5D) atom; ^{2,4}Contracted and uncontracted basis sets for O (^3P) atom.

^{5,6}Contracted and uncontracted basis sets for Gd (^7F) atom.

The properties of polyatomic systems are best described when polarization functions are included in the

basis sets used in calculations with these systems. As for GdFeO_3 , the polarization function was considered in the

[4s2p] basis set for O (3P) atom. It was extracted from de primitive basis set. The adequate exponent was chosen through successive calculations for $GdFeO_3$ by using different primitive functions, taking into account the minimum energy criterion at DKH second-order scalar relativistic level. The polarization function obtained by this strategy is $\alpha_d = 0.396928$.

In order to describe the configuration of a metal in a polyatomic system it is necessary to include diffuse functions in the basis set for the metal. The configurations of the metals in $GdFeO_3$ were adequately described by adding a function by symmetry to the basis set of each metal atom. The diffuse functions obtained through the total energy optimization of the ground state anions Fe^{1-} and Gd^{1-} by GCHF method. For the 12s6p5d and 19s12p8d4f basis sets, the diffuse functions are: $\alpha_s = 0.0145512$; $\alpha_p = 0.115324$; $\alpha_d = 0.0538269$ and $\alpha_s = 0.00873780$; $\alpha_p = 0.0617874$; $\alpha_d = 0.262367$; $\alpha_f = 0.118836$, respectively.

In this work, atomic calculations (contraction of the basis sets and choice of diffuse functions) were performed with the ATOMSCF program [21], while calculations with molecular systems were carried out with the Gaussian program [22].

III. RESULTS AND DISCUSSION

Before starting the presentation and discussion of the results obtained in the investigation of piezoelectricity in $GdFeO_3$, objective of this work, it is important to note some considerations about the fragment model that was used in the representation of the crystalline system under study.

Fig. 1 shows the fragments we have used as a model to simulate the conditions necessary to the existence of piezoelectricity in ABO_3 perovskites [11, 12, 23, 24]. In Fig. 1 (A); (a) represents the $[GdFeO_3]_2$ fragment having the Fe atoms fixed in the space; (b) represents the $[GdFeO_3]_2$ fragment in which the Fe atoms are being moved $+0.005 \text{ \AA}$ in the symmetry X axis, while the Gd and O atoms are maintained fixed; (c) represents the $[GdFeO_3]_2$ fragment in which the Fe atoms are moved -0.005 \AA in the symmetry X axis and Gd and O atoms are maintained fixed. Fig. 1 (B) represents the $[GdFeO_3]_2$ fragment having the bond lengths $r(Fe_1O_3)$, $r(Fe_1O_4)$, $r(Fe_2O_4)$ shortened in 0.005 \AA . The same fragment model was used in the study developed with $SmTiO_3$ [11], $YFeO_3$ [12], $BaTiO_3$ [23] and also in investigations with $LaFeO_3$ [24]. In this report, the model represents the crystalline 3D periodic $GdFeO_3$ system. The Fe atom is located in the center of the

octahedron, being wrapped up by six O atoms arranged in the reticular plane (200) and two Gd atoms arranged in the reticular plane (100).

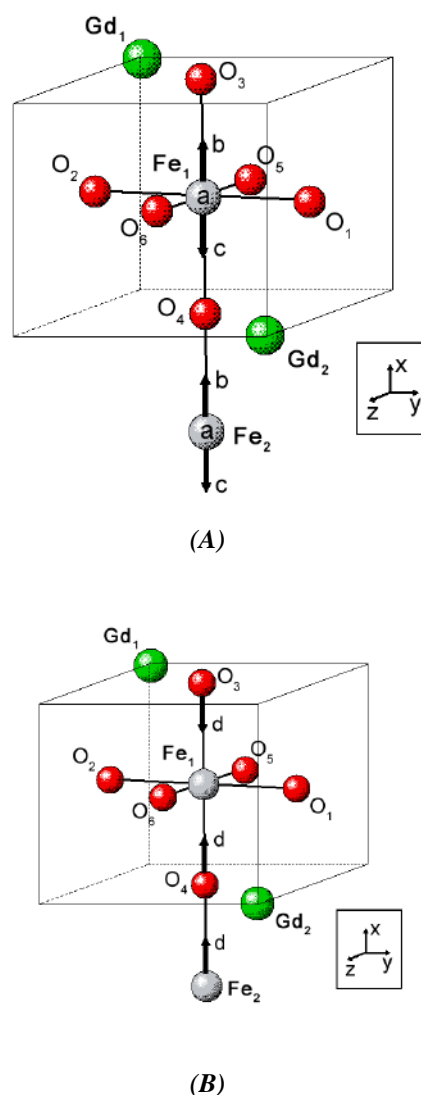


Fig. 1. The octahedral $[GdFeO_3]_2$ fragment. (A): (a) represents the $[GdFeO_3]_2$ fragment having the Fe atoms fixed in the space; (b) represents the $[GdFeO_3]_2$ fragment in which the Fe atoms are being moved $+0.005 \text{ \AA}$ in the symmetry X axis, while the Gd and O atoms are maintained fixed; (c) represents the $[GdFeO_3]_2$ fragment in which the Fe atoms are moved -0.005 \AA symmetry X axis and Gd and O atoms are maintained fixed; (B): represents the $[GdFeO_3]_2$ fragment having the bond lengths $r(Fe_1O_3)$, $r(Fe_1O_4)$, and $r(Fe_2O_4)$ shortened from 0.005 \AA

It is important to note that in order to study the crystalline 3D periodic $GdFeO_3$ system it is necessary to choose a fragment, a molecular model, capable of adequately represent the physical property of the crystalline system as whole.

We still would like to point out three very important strategic aspects in our theoretical approach in the study of gadolinium ferrite piezoelectricity, namely: (i) Firstly, we consider that the piezoelectric properties in GdFeO_3 result from uncentrosymmetric characteristics presented by central ion and the probable polarization of the crystal when submitted to mechanical stress. (ii) Secondly, the geometry optimization of the $[\text{GdFeO}_3]_2$ fragment in the C_s symmetry and electronic state $^1A'$ was carried out. (iii) Finally, single-point calculations were performed with the optimized geometry, according to the descriptions shown in Fig.1, and their results were analyzed from the point of view of strategy (i).

We will now return to the presentation and discussion of the results obtained in this study with the

Table 2. Theoretical and experimental bond length (\AA) for $^1\text{FeO}^{1+}$ and $^1\text{GdO}^{1+}$ molecular fragments

Bond length			
Molecular fragment	Theoretical	Experimental [25]	Δr
$r(^1\text{FeO}^{1+})$	1.9063	1.9495	4.32×10^{-2}
$r(^1\text{GdO}^{1+})$	2.1852	2.2652	8.00×10^{-2}

$$\Delta r = |\text{Theoretical} - \text{Experimental}|$$

TABLE 3 presents the dipole moment and the TER energy of the $[\text{GdFeO}_3]_2$ fragment. It can be seen from this table that the result with Fe^{3+} central ion at (b) or (c) is 0.014 and 0.35 hartree, respectively, more stable than at (a), pointing out that the Fe^{3+} central ion is not centrosymmetric. This evidence is confirmed by the decrease in dipole moment at positions (b) and (c) when compared to the Fe^{3+} central ion position at (a). In addition, the table also shows that the

Table 3. Dipole moment (D) e TER (hartree) of the $[\text{GdFeO}_3]_2$ fragment

Fe atom position	μ_x	μ_y	μ_z	μ	TRE
(a)	-0.25	4.19	2.08	7.61	-24609.25295
(b)	-0.613	-1.86	1.87	7.46	-24609.26693
(c)	-2.04	0.718	0.0311	2.16	-24609.60649
(d)	2.99	3.51	1.14	4.75	-24609.66129

TABLE 4 shows the total atomic charges of the $[\text{GdFeO}_3]_2$ fragment when Fe^{3+} central ion is at positions (a), (b), and (c), and for the shortened $r(\text{Fe}_1\text{O}_3)$, $r(\text{Fe}_1\text{O}_4)$, and $r(\text{Fe}_2\text{O}_4)$ bond lengths, position (d). In this table, when the Fe^{3+} ion central is moved to position (b), atomic charges migrate from the Fe_2 , Gd_1 , and Gd_2 atoms to the O_2 , O_3 , O_4 , O_5 , and O_6 atoms. On the other hand, when the Fe^{3+} central ion is moved to position (c), a migration of atomic charges from

perovskite GdFeO_3 . Initially, we would like to highlight the comparison of calculated and experimental bond length (r) values [25] and then examine the quality of the contracted basis set supplemented with polarization function and diffuse functions, $[4s2p1d]/[13s7p6d]/[20s13p9d5f]$, in describing the geometry of the system under investigation. In TABLE 2, we show and compare results for $r(^1\text{FeO}^{1+})$ and $r(^1\text{GdO}^{1+})$. In this table, the theoretical results reproduce very well the experimental values with differences (Δr) of $4.32 \times 10^{-2} \text{\AA}$ and $8.00 \times 10^{-2} \text{\AA}$, respectively, showing the good performance of the molecular $[4s2p1d]/[13s7p6d]/[20s13p9d5f]$ basis set in the description of the geometry of the $[\text{GdFeO}_3]_2$ fragment studied.

decrease in $r(\text{Fe}_1\text{O}_3)$, $r(\text{Fe}_1\text{O}_4)$, and $r(\text{Fe}_2\text{O}_4)$ bond lengths, the calculations at the atomic position (d), provoke a migration of atomic charges among the atoms of the $[\text{GdFeO}_3]_2$ fragment and, consequently, a decrease of the dipole moment. These results suggest that there is a probable polarization of the GdFeO_3 crystal when submitted to mechanical stress.

the Fe_2 , Gd_1 , and Gd_2 atoms to the O_2 , O_3 , O_5 , and O_6 atoms also occurs. Shortened $r(\text{Fe}_1\text{O}_3)$, $r(\text{Fe}_1\text{O}_4)$, and $r(\text{Fe}_2\text{O}_4)$ bond lengths, position (d) provoke a charge migration from the Fe_2 , Gd_1 , and Gd_2 atoms to the O_2 , O_5 , and O_6 atoms. We can notice that, according to TABLE 4, the oscillation of the Fe^{3+} central ion and the shortening of the bond lengths caused by mechanical stress provokes a rearrangement of the total charges on atoms compared with

the position (a) of the $[\text{GdFeO}_3]_2$ fragment. The rearrangement of the charges at (d) as well as the decrease of the dipole moment can lead us to suppose that the decrease of $r(\text{Fe}_1\text{O}_3)$, $r(\text{Fe}_1\text{O}_4)$, and $r(\text{Fe}_2\text{O}_4)$ bond lengths provokes a polarization of the $[\text{GdFeO}_3]_2$ fragment. We can also report that the electron density does not change significantly at atomic positions (b) and (c) – the Fe^{3+} central ion is deviated from the main axis of X symmetry – when compared with the atomic position (a). This is an indication that the nature of Fe-O and Gd-O chemical bonds does not change when the Fe^{3+} central ion deviates from the X symmetry of the $[\text{GdFeO}_3]_2$ fragment. At (d) position, the decrease of the $r(\text{Fe}_1\text{O}_3)$, $r(\text{Fe}_1\text{O}_4)$, and $r(\text{Fe}_2\text{O}_4)$ bond lengths provokes the deviation of electronic density in the $[\text{GdFeO}_3]_2$ fragment, indicating the nature of the Fe-O and Gd-O chemical bonds was altered.

Table 4. Total atomic charges from $[\text{GdFeO}_3]_2$ fragment

Atom	Atom position			
	(a)	(b)	(c)	(d)
Fe_1	1.60	1.57	1.49	1.48
Fe_2	0.339	0.551	0.571	0.584
Gd_1	1.32	1.68	1.41	1.42
Gd_2	1.21	1.38	1.39	1.43
O_1	-1.06	-0.652	-0.974	-0.979
O_2	-1.32	-1.34	-1.49	-1.49
O_3	-0.247	-0.267	-0.284	-0.168
O_4	-0.416	-0.779	-0.122	-0.359
O_5	-0.968	-0.973	-0.984	-0.97
O_6	-0.864	-0.870	-0.953	-0.949

Thus, we can notice that electrostatic interactions play an important role in the constitution of the electronic structure of the $[\text{GdFeO}_3]_2$ fragment. This is consistent for two reasons, namely: (1) due to the repulsive effect of d and f electrons in both high-spin and low-spin octahedral species of ML complexes (M=metal and L=ligand), all d and f electrons density will repel the bonding electrons density [26]; (2) in lanthanide complexes, chemical bonds of ionic nature predominate [27].

Analysis of the oscillation of the Fe^{3+} central ion between the positions (b) and (c), and the shortening of the $r(\text{Fe}_1\text{O}_3)$, $r(\text{Fe}_1\text{O}_4)$, and $r(\text{Fe}_2\text{O}_4)$ bond lengths in the $[\text{GdFeO}_3]_2$ fragment, position (d), showed that the occurrence of the uncentrosymmetrical-centered cation (Fe^{3+}) and the polarization of the $[\text{GdFeO}_3]_2$ fragment produce an electric current, leading us

to infer in this work evidence that GdFeO_3 may present piezoelectricity caused by electrostatic interactions of its atoms.

IV. CONCLUDING REMARKS

The use of DKH second-order scalar relativistic approach together with qualified basis sets to represent the GdFeO_3 polyatomic system allowed the simulation of the conditions necessary for the existence of piezoelectricity in this material. The calculated properties allow us to infer that:

1. The Fe^{3+} central ion in the $[\text{GdFeO}_3]_2$ fragment has uncentrosymmetrical characteristics. In addition, when submitted to mechanical stress, the $[\text{GdFeO}_3]_2$ fragment presents polarization, which leads us to suggest the existence of piezoelectricity in GdFeO_3 , caused by electrostatic interactions.

2. The results of the computational investigation presented in this work, punctuating the possible piezoelectricity in GdFeO_3 through the use of the fragment model used to investigate this property in BaTiO_3 , LaTiO_3 , and SmTiO_3 corroborate the viability of the model and methodology to investigate possible piezoelectricity in other ABO_3 perovskites.

ACKNOWLEDGEMENTS

We gratefully acknowledge the financial support from Brazilian agencies Conselho Nacional de Desenvolvimento Científico e Tecnológico (CNPq) and Coordenação de Aperfeiçoamento de Pessoal de Nível Superior (CAPES). We employed computing facilities at the Theoretical and Computational Chemistry Laboratory (LQTC) of the Universidade Federal do Pará (UFPA) and High-Performance Processing National Center (CENAPAD) of the Universidade Estadual de Campinas (UNICAMP).

This work is dedicated to Professor José Raymundo Ribeiro Serra (in memoriam). Professor Serra was one of the creators of the Post-Graduation Course in Chemistry and contributed to the formation of many generations of chemists, physicists, geologists, pharmacists and engineers at the Chemistry Department of the Universidade Federal do Pará.

REFERENCES

- [1] Roberts, S. (1947). Dielectric and piezoelectric properties of barium titanate. *Phys. Rev.* 71:890-895. [10.1103/PhysRev.71.890](https://doi.org/10.1103/PhysRev.71.890).

- [2] Assirey, E. A. R. (2019). Perovskite synthesis, properties and their related biochemical and industrial application. Saudi. Pharm.J. 27:817-819.DOI:10.1016/j.jsps.2019.05.003.
- [3] Kot, M., Das.C., Baran, D., Saliba, M. (2019). Themed issue on electronic properties and characterization of perovskites. J. Mater. Chem. C 7:524-525. DOI:10.1039/c9tc90085c.
- [4] Uchino, K. (2015). Glory of piezoelectric perovskite. Sci. Technol. Adv. Mater. 16:1-16. DOI: 10.1088/1468-6996/16/4/046001.
- [5] Bhalla, A. S., Guo, R., Roy, R. (2000). The perovskite structure – a review of its role in ceramic science and technology. Mat. Res. Innovat.4: 3-26. ISSN: 1432-8917.
- [6] Tejuca, J. L., Fierro, J. L. G. (1993). Properties and Applications of Perovskite- Type Oxides. Marcel Dekker, New York. ISBN: 0824787862 9780824787868.
- [7] Müller, K. A., Kol, T. W. (2010). Properties of Perovskites and Other Oxides. World Scientific, Singapore. DOI: 10.1080/00107514.2912.657688.
- [8] Cady, G. (1964). Piezoelectricity. McGraw-Hill, New York. ISBN: 0486838603.
- [9] Goldschmidt, V. M. (1926). Crystal structure of rutile type with remarks on the geochemistry of the bivalente and quadrivalent elements. Skrifter Norske Videnskaps – Akad. Oslo I. Mat-Naturv K1 2: 8.
- [10] Jaffe, B., Cook, W. R. Jr., Jaffe, H. (1971). Piezoelectric Ceramics. Academic Press, New York. DOI: 10.1016/0022-460X(72)90684-0.
- [11] Costa, E. B., Farias, M. S., Miranda, R. M., Dos Santos, M. A. B., Lobato, M. S., De Figueiredo, A. F., Ferreira, R. D. P., Gil, F. S., Pinheiro, J. C., Treu-Filho, O., Kondo, R. T. (2009). Na insight into the theoretical investigation of possible piezoelectric effect in samarium titanate (SmTiO₃). Comput. Mater. Sci. 44: 1150-1152. DOI: 10.1016/j.commatsci.2008.07.028.
- [12] Lira, F. A. M., Farias, M. S., Figueiredo, A. F., Gil, F. S., Dos Santos, M. A. B., Malheiros, B. V., Ferreira, J. E. V., Pinheiro, J. C., Treu-Filho, O., Kondo, R. T. (2011). Quantum mechanical modeling of perovskite: An investigation of piezoelectricity in ferrite yttrium. J. Mol. Model. 17:1621-1624. DOI: 10.1007/s00894-010-0797-2.
- [13] Aquino, E. L. C., Santos, M. B., Farias, M. S., Alves, S. S., Gil, F. S., De Figueiredo, A. F., Lobato, J. R. B., Ferreira, R. D. P., Treu-Filho, O., Kondo, R. T., Pinheiro, J. C. (1916). Quantum Mechanical Approahes for Piezoelectricity Study in Perovskites. In: Ogawa T (Ed). Piezoelectric Materials. Intech Open, Croatia, pp 64-82. DOI:10.5772/62696.
- [14] Mohallem, J. R., Dreizler, R. M., Trsic, M. (1986). A Griffin Hill-Wheeler version of the Hartree-Fock Equations. Int. J. Quant. Chem. Symp. 20: 45-55. DOI: 10.1002/qua.560300707.
- [15] Mohallem, J. R., Trsic, M. (1987). A universal Gaussian basis set for Li through Ne based on a generator coordinate version of the Hartree-Fock equations. J. Chem. Phys. 86: 5043-5044. DOI: 10.1063/1.452680.
- [16] Trsic, M., Silva, A. B. F. (2017). Electronic Atomic and Molecular Calculations Applying the Generator Coordinate Method. Elsevier, New York. ISBN: 978-0-444-52781-3.
- [17] Douglas, M., Kroll, N. M. (1974). Quantum electrodynamical corrections to the fine structure of helium. Ann. Phys. 82: 89-155. DOI:10.1016/0003-4916(74)90333-9.
- [18] Hess, B. A. (1985). Applicability of the no-pair equation with free-particle projection operators to atomic and molecular structure calculations. Phys. Rev. A 32: 756-763. DOI: 10.1103/physreva.32.756.
- [19] Hess, B. A. (1986). Relativistic electronic-structure calculations employing a two-component no-pair formalism with external-field projection operators. Phys. Rev. A 33: 3742-3748. DOI:10.1103/PhysRevA.33.3742.
- [20] Dunning, T. H. Jr., Hey, P. J. (1997). Modern Theoretical Chemistry. In: Schaefer II HF (Ed) Methods of Electronic Structure Theory. Plenum, New York. ISBN-13: 978-1475708899.
- [21] Pavani, R., Clementi, E. (1989). Tech Rep RJ. IBM, New York
- [22] Fisch, M. J., Trucks, G. W., Schlegel, H. B., Gill, P. M. W., Johnson, B. G., Robb, M. A., Cheeseman, J. R., Keith, T. A., Peterson, G. A., Montgomery, J. A., Raghavachari, K., Al-Laham, M. A., Zakrzewski, V. G., Ortiz, J. V., Foresman, J. B., Cioslowski, J., Stefanov, B. B., Nanayakkara, A., Challacombe, M., Peng, C. Y., Ayala, P. Y., Cheng, W., Wong, M. W., Andres, J. L., Replogle, E. S., Gomperts, R., Martin, R. L., Fox, D. J., Binkley, J. S., Defrees, D. J., Baker, J., Stewart, J. P., Head-Gordon, M., Gonzalez, C., Pople, J. (2004) Gaussian 03, Revision D 01. Gaussian Inc, Pittsburgh.
- [23] Treu-Filho, O., Pinheiro, J. C., Kondo, R. T. (2004). Designing Gaussian basis sets to thee theoretical study of the piezoelectric effect of perovskite (BaTiO₃). J. Mol. Struct. (Theochem) 671:71-75. DOI: 10.1016/j.theochem.2003.10.032.
- [24] Santos, C. C., Barbosa, J. P., Santos, M. A. B., Lira, F. A. M., Cardoso, F. J. B., Pinheiro, J. C., Treu-Filho, O., Kondo, R. T. (2007). Investigation of perovskite (LaFeO₃): A theoretical study. Comput. Mater. Sci. 39:713-717. DOI: 10.1016/j.commatsci.2006.09.004.
- [25] Coppens, P., Eibschütz, M. (1965). Determination of the Crystal Structure of Yttrium Orthoferrite and Refinement of Gadolinium Orthoferrite. Acta Cryst. 19:524-531. DOI:10.1107/S0365110X65003833.
- [26] Gerloch, M., Contable, E. C. (1994). Transition Metal Chemistry. VCH, Weinheim. ISBN: 978-3527292196.
- [27] Kaltsoyannis, N., Scott, P. (1999). The f Elements. Oxford University Press, Oxford. ISBN: 9780198504672.